ISSN: 2476-6909; Modares. Mech. Eng. *2026;26(04):261-269.*

Modares Mechanical Engineering

DOI: 10.48311/mme.2026.118299.82908
journal homepage: mme.modares.ac.ir

Design, Control, and Experimental Evaluation of a Lightweight Active Knee–Ankle–Foot Orthosis with Adjustable Knee Motion for Mobility Assistance After Spinal Cord Injury

Sahand Hosseinpour Malakouti, Sajjad Ozgoli*

Electrical and Computer Engineering Department, Tarbiat Modares University, Tehran, Iran

ARTICLE INFO

Article Type
Original Research

Article History
Received: December 16, 2025
Revised: January 14, 2026
Accepted: October 31, 2025
ePublished: February 16, 2026

ABSTRACT

For individuals with spinal cord injury (SCI) who walk with conventional knee–ankle–foot orthoses (KAFOs), locked knees and compensatory trunk and upper-limb motions can limit gait efficiency. This study presents a lightweight active KAFO that provides powered knee assistance while still being used like a conventional KAFO. The device integrates a back drivable knee actuator within a two-level control architecture: a high-level controller, comprising a finite state machine and a parametric trajectory generator that computes the knee reference from user-selected step height and speed, and a low-level position-based impedance controller tracks this trajectory. Step height and speed can be adjusted in real time via an on-board touchscreen interface, and a ramp-based timing strategy allows smooth changes in gait cycle duration over roughly a two-fold range. A pilot case study was conducted on a single adult with chronic incomplete SCI who walks with KAFOs and a walker. Two configurations were compared: his usual conventional KAFO set-up and one with the proposed active KAFO. Clinical outcome measures included the 10m walking test (10MWT), the 6 min walking test (6MWT) and end-of-test heart rate. With the active KAFO, the participant achieved a higher 10MWT walking speed than with his conventional KAFOs, whereas no clear difference was observed in 6MWT distance and heart rate responses remained in a similar range. These preliminary results suggest that an active KAFO with an adjustable knee trajectory and on-board tuning of gait parameters may offer a feasible intermediate option between conventional KAFOs and full lower-limb exoskeletons.

Keywords: Spinal cord injury, Powered knee exoskeleton, knee–ankle–foot orthosis, Rehabilitation robotics, Clinical case study

How to cite this article
Hosseinpour Malakouti S, Ozgoli S, Design, Control, and Experimental Evaluation of a Lightweight Active Knee–Ankle–Foot Orthosis with Adjustable Knee Motion for Mobility Assistance After Spinal Cord Injury. Modares Mechanical Engineering. *2026;26(04):261-269.*

**Corresponding author's email: Ozgoli@modares.ac.ir*
**Corresponding ORCID ID: 0000-0001-8567-1679*

شاپا: ۷۹۰۹-۲۴۷۶؛ مهندسی مکانیک مدرس. ۲۶۹-۲۶۱:(۰۴)۲۶;۱۴۰۵

مهندسی مکانیک مدرس

DOI: 10.48311/mme.2026.118299.82908

صفحه اصلی مجله: mme.modares.ac.ir

طراحی، کنترل و ارزیابی عملی ارتز فعال زانو با الگوی حرکتی قابل تنظیم جهت کمک به افراد دچار آسیب نخاعی

سهند حسین‌پور ملکوتی، سجّاد ازگلی*

گروه مهندسی برق و کامپیوتر، دانشگاه تربیت مدرس، تهران، ایران

اطلاعات مقاله

نوع مقاله
مقاله پژوهشی

تاریخچه مقاله
دریافت: ۱۴۰۴/۰۹/۲۵
بازنگری: ۱۴۰۴/۱۰/۲۴
پذیرش: ۱۴۰۴/۱۱/۰۸
ارائه آنلاین: ۱۴۰۴/۱۱/۲۷

چکیده

در افراد آسیب نخاعی که برای راه رفتن از ارتزهای سنتی استفاده می‌کنند، قفل بودن زانو باعث فاصله گرفتن الگوی حرکتی از حالت طبیعی شده و این امر باعث کاهش راندمان و افزایش خستگی در فرد می‌گردد. برای حل این مشکل، در این پژوهش یک ارتز فعالِ سبک با عملگر الکتریکی فشرده در مفصل زانو معرفی شده است. راهبرد کنترل این ارتز به‌صورت سلسله‌مراتبی و دو سطحی است. به این‌صورت که در کنترل سطح بالا، یک ماشین حالت وظیفه‌ی مدیریت وضعیت‌های مختلف کاربر را برعهده داشته و در کنار آن یک تولیدکننده‌ی مسیر با توجه به متغیرهای انتخاب‌شده توسط کاربر مسیر مرجع زانو را تولید می‌کند. در این بخش، برای اعمال تغییرات مدنظر در متغیر سرعت، از روش زمان‌بندی تدریجی (رمپ سرعت) جهت پیوستگی و نرمی حرکت زانو استفاده شده است. در کنترل سطح پایین، کنترل‌کننده‌ی امپدانسی مبتنی بر موقعیت به‌منظور دنبال‌کردن مسیر مرجع، مستقر است. برای ارزیابی عملکرد، مطالعه‌ای روی فرد آسیب نخاعی در دو وضعیت پوشیدن ارتز سنتی و ارتز فعال پیشنهادی با شاخص‌های بالینی رایج (آزمون ۱۰ متر و آزمون ۶ دقیقه) انجام گردید. نتایج نشان داد که با استفاده از ارتز فعال، سرعت راه‌رفتن فرد در آزمون ۱۰ متر افزایش قابل توجهی می‌یابد در حالی‌که مسافت طی‌شده برای دو تجهیز در آزمون ۶ دقیقه مشابه بوده و تغییرات ضربان قلب نیز در محدوده‌ی مجاز باقی ماند. نتایج مقدماتی نشان می‌دهد که ارتز فعال زانو با امکان تنظیم الگوی حرکتی می‌تواند به‌عنوان یک راهکار میانی و بین ارتزهای سنتی و اسکلت‌های بیرونی کامل اندام تحتانی مطرح شود.

کلیدواژه‌ها: آسیب نخاعی، اسکلت بیرونی، ارتز فعال زانو، توانبخشی، کارآزمایی بالینی

نحوه ارجاع به این مقاله

حسین‌پور ملکوتی سهند، ازگلی سجاد، طراحی، کنترل و ارزیابی عملی ارتز فعال زانو با الگوی حرکتی قابل تنظیم جهت کمک به افراد دچار آسیب نخاعی ، مهندسی مکانیک مدرس. ۲۶۹-۲۶۱:(۰۴)۲۶;۱۴۰۵

*پست الکترونیکی نویسنده عهده‌دار مکاتبات: ozgoli@modares.ac.ir

*شناسه ارکید نویسنده عهده‌دار مکاتبات: 0000-0001-8567-1679

1- Introduction

Spinal cord injury (SCI) is a life-altering condition that often results in partial or complete paralysis and loss of sensation below the level of injury. Following SCI, most individuals rely on wheelchairs for mobility, which restores basic locomotion but leads to prolonged sitting and a largely sedentary lifestyle. Over time, this immobility contributes to numerous secondary complications, such as chronic pain, spasticity, bowel and bladder dysfunction, muscle atrophy, osteoporosis, and cardiovascular deconditioning that markedly reduce health and quality of life [1]. Globally, SCI affects a large population: recent epidemiological analyses estimate around 20 million people living with SCI worldwide, with close to 1 million new cases each year. Roughly 22% of individuals with SCI are classified as having incomplete paraplegia, meaning that some motor and/or sensory function is preserved below the level of injury [2]. Many individuals in this group have the potential to stand and walk using assistive devices, making them suitable candidates for gait-support technologies, even if they are not fully independent [3].

A wide range of assistive devices is available for people with SCI. Conventional orthoses such as knee–ankle–foot orthoses (KAFOs) enable standing and walking by locking the lower-limb joints in a stable, extended position [4]. While these braces provide essential stability, they severely restrict joint range of motion and force users to rely heavily on their upper limbs, often leading to compensatory movements, shoulder pain, rapid fatigue, and an inefficient, unnatural gait pattern [5]. To address the limitations of passive bracing, powered lower-limb exoskeletons have been developed as a high-tech alternative that can actively move the lower-limb joints to produce a more physiological gait pattern. Beyond restoring walking ability, exoskeleton-assisted training has been linked to reduced spasticity, improved psychological well-being, and positive effects on bone density, cardiovascular health, and bowel function [6-8]. However, current systems are typically bulky and heavy, expensive, difficult to don and doff, and still require substantial upper-limb support and supervision, which makes them poorly suited for unsupervised, everyday use in the community [9, 10]. Moreover, clinical trials directly comparing exoskeleton-assisted gait with KAFO-based walking in people with SCI report improved kinematics and, in some cases, reduced energy cost, but generally similar walking distances, speeds, and usability ratings, so current exoskeletons cannot yet be regarded as a universally preferable alternative to conventional orthoses [11, 12].

To bridge the gap between simple passive bracing and complex powered exoskeletons, researchers have proposed active KAFOs and knee-focused exoskeletons for individuals with incomplete SCI who retain sufficient trunk stability and some residual hip control [13, 14]. These devices are designed to provide reliable knee support during stance while actively generating controlled knee flexion–extension during swing, with the aim of improving gait quality without complexity, high cost, and bulk of a full lower-limb exoskeleton. Several concepts and prototypes have been reported, targeting either rehabilitation training or functional assistance during walking.

Based on this body of work, existing active KAFOs and knee exoskeletons can be broadly classified into two categories. The first group comprises torque- or impedance-based controllers, which generate assistive knee torque as a function of gait phase or neuromuscular model outputs without prescribing an explicit knee angle trajectory. Devices in this category include the Marsi Active Knee [15] which uses a rotary series elastic actuator at the knee within a finite-state impedance controller. The SUT-KneeExo [16] exoskeleton provides another example of a series-elastic-actuator-driven device with a fuzzy output-feedback assistive controller that reduces muscle activation while tracking normative knee motion. The ABLE-KS unilateral knee exoskeleton [17] similarly uses a finite-state controller driven by joint sensors and inertial units to modulate knee support across stance and swing. Neuromuscular-inspired approaches such as the Symbitron exoskeleton [18], generate knee torques online via virtual muscles based on joint kinematics and ground contact, while backdrivable unloading modules like M-BLUE [19] use low-impedance current-based torque control to compensate a fraction of the user's body weight without prescribing joint trajectories. These systems have reported improvements in knee kinematics, walking capacity, or muscle effort in small cohorts of stroke or incomplete SCI users, or in single-subject experiments with healthy participants, but are typically evaluated in constrained laboratory environments such as treadmills or parallel bars.

The second group comprises trajectory-tracking controllers, which define a desired knee angle trajectory and use joint-space PD controller or impedance control to follow it. Parametric models of constrained human gait have also been proposed for lower-limb active orthosis, in which joint trajectories are expressed as analytic functions of stride length, step height, walking speed, and limb segment lengths and then implemented on an assistive exoskeleton platform [20]. The bilateral ABLE orthosis [21], for example, augments a stance-control KAFO with a motorized knee that tracks a parametric swing trajectory tuned via a PC interface to match the user's motor capacity. In a single participant with incomplete SCI, this device has shown faster, more symmetric gait with increased hip–knee range of motion compared with locked passive KAFOs. Complementary simulation studies have used planar musculoskeletal models [22] and optimal control formulations [23] to identify knee torque patterns and peak-flexion trajectories that could improve gait kinematics, foot clearance, and orthosis effort for different incomplete-SCI severities. However, these predicted patterns have not been implemented in real-time controllers or tested in overground clinical scenarios. Although both torque-based and trajectory-tracking strategies have demonstrated promising acute effects, the devices reviewed above mostly rely on IMU-based gait-event detection. This may be unreliable in users with severely impaired lower-limb mobility.

Furthermore, in many of these systems, knee-motion tuning is exposed through research-oriented PC interfaces rather than simple on-device tools. Moreover, evaluations are largely restricted to laboratory settings, which limits their relevance to everyday KAFO users.

In this work, we address these gaps by developing a lightweight, backdrivable active KAFO that retrofits a quasi-direct-drive knee actuator onto a conventional rigid KAFO and implements a richer state machine encompassing level walking, sit-to-stand and stand-to-sit transitions, and seated knee-training modes. We introduce a handheld interface through which both the user and therapist can tune key knee-trajectory parameters during use. The torque-controlled actuator is driven by a joint-space PD impedance controller around a predefined, user-specific knee angle trajectory.

The remainder of this paper is organized as follows. Section 2 details the active KAFO hardware and its mechanical integration with a conventional rigid brace, the finite state machine that coordinates walking and transitional modes, the embedded control framework and joint-space impedance controller, and the experimental protocol and outcome measures. Section 3 presents and discusses the results of the single-case study. Section 4 concludes the paper and outlines limitations and directions for future work.

2- Device Design, Control, and Experimental Methods

This section describes the design and implementation of the proposed active KAFO, including actuator selection and electronics architecture, mechanical integration with a conventional rigid orthosis and the overall control framework. We then introduce the parameterized knee motion pattern and its on-device tuning interface, which together enable practical deployment and adjustment of the system in clinical and everyday settings.

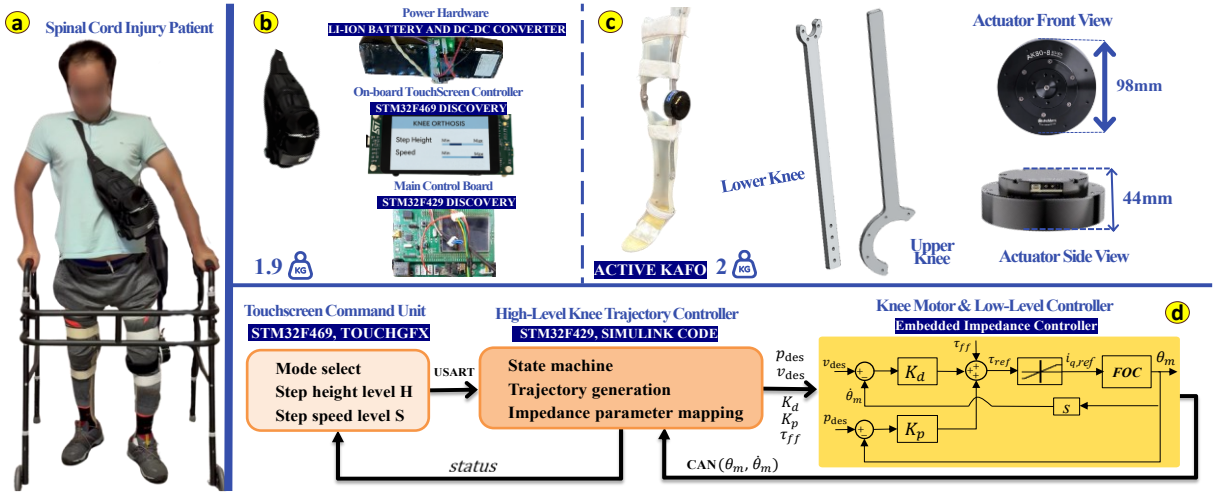

Fig.1 Overview of the active KAFO system. (a) Spinal cord injury participant walking overground with the active KAFO. (b) Electronic components integrated in a compact cross-body sling bag. (c) Knee actuator dimensions with custom thigh and shank links. (d) Control architecture with touchscreen interface, high-level trajectory generator, and low-level impedance controller.

2-1- Actuation and Embedded Electronics

The knee joint is actuated by a commercially available T-Motor AK80-8 unit [24] with a 1:8 internal transmission; its dimensional layout is illustrated in Fig. 1(c) and its main specifications are listed in Table 1. The actuator has a low total mass, which helps keep the overall KAFO weight low—a critical factor for comfort and everyday usability. Due to its low backdrive torque (0.75 Nm at the output), the actuator allows the joint to be moved by the user with minimal resistance, facilitating active knee motion in users with incomplete SCI. Even though its torque is less than that of some other knee exoskeleton actuators, it is well aligned with the needs of our target users, who preserve partial lower-limb function and typically offload a significant fraction of body weight via a walker or comparable assistive aid during ambulation.

Table 1 Main specifications of the knee actuator (T-Motor AK80-8)

Weight (g)	**570**
Peak Torque (Nm)	**30**
Rated speed (rpm)	**243**
Range of Motion (degree)	**-120 to 5**
BackDrive Torque (Nm)	**0.75**

To enable autonomous operation outside laboratory settings, the active KAFO integrates all required electronics, power, and user-interface components in a compact wearable setup, as summarized below. All electronic components are integrated in a compact cross-body sling bag, as shown in Fig. 1(b). Power is provided by a 44.4 V Li-ion battery (5 Ah capacity), which is connected to a power board supplying the knee actuator at voltage (48 V) and generating a regulated 5V for the low-power electronics. The main controller is an STM32F429 Discovery board, which handles communication with the actuator over a CAN bus and with the hand-held terminal via a USART link. An additional touchscreen hand terminal based on an STM32F469 platform is used to display the orthosis status and to send user commands and gait-parameter settings; its graphical user interface was implemented using the TouchGFX framework. As implemented, the on-leg mass of the active KAFO (including the actuator and mechanical additions) is approximately 2.0 kg, whereas all electronic components, including the battery, have a combined mass of about 1.5 kg carried in the cross-body bag. The state-machine structure and the high-level/low-level control algorithms executed on the main controller are detailed in the following subsections.

2-2- Mechanical integration

To ensure practical deployment, the proposed system was conceived as a retrofit add-on to the user's conventional KAFO. Therefore, the mechanical interface between the actuator and the orthosis was explicitly designed based on the subject-specific geometry of the brace. A 3D model of the participant's KAFO was first generated, including the thigh, shank, and foot shells as well as the medial free-motion knee joint. Two output links (thigh and shank links) were then designed to couple the actuator to the outer side of the KAFO knee joint, as illustrated in Fig. 2. The link geometry was selected to preserve the required knee range of motion reported in Table 1 while mechanically limiting excessive extension to prevent hyperextension. After the initial layout, the link shapes were refined to improve conformity with the orthosis contours and joint alignment, providing adequate clearance and a compact integration. The resulting interface concept was also intended to be applicable to either limb (left or right) with the same linkage design.

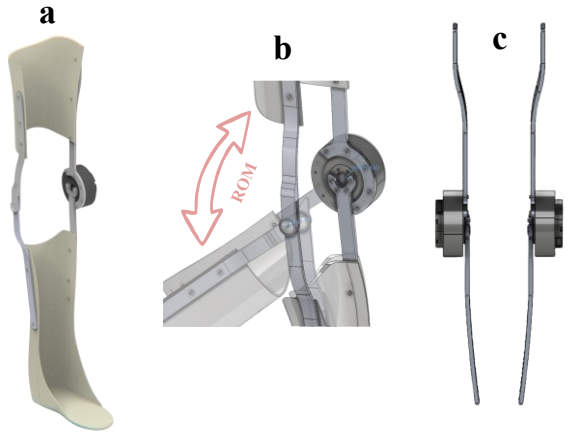

Fig. 2 Mechanical integration of the retrofit actuator with the subject-specific thermoplastic KAFO: (a) 3D model of the custom orthosis, (b) achieved knee range of motion (ROM) and (c) refined thigh and shank link geometries for improved conformity and alignment with the brace.

To verify the structural integrity of the designed links, a static finite-element analysis (FEA) was performed in ANSYS for the shank link (B) and the thigh link (A) in Fig 3. The links were modeled using aluminum alloy 7075, and the von-Mises equivalent stress criterion was adopted. The loading condition was defined by applying a 30 N·m torsional moment about the knee axis at the actuator–link interface,

while the remaining interfaces were constrained to represent attachment to the orthosis. The safety factor was computed on a yield basis as the ratio between the material yield strength and the von-Mises equivalent stress.

Fig. 3 reports the resulting safety factor and total deformation distributions for both links. Under the above loading, the minimum safety factor was ≈1.48 for the shank link (B) and ≈1.26 for the thigh link (A). The maximum total deformation remained below 1 mm, reaching ≈0.58 mm for the shank link and ≈0.77 mm for the thigh link. Overall, these results indicate that the proposed links provide sufficient strength and stiffness for the intended assisted-walking application.

After finalizing the geometry, the links were manufactured from 6-mm aluminum 7075 sheet (no heat treatment) using a laser-cutting process and were subsequently formed and adjusted to match the subject-specific thermoplastic KAFO contours for accurate fitting and alignment.

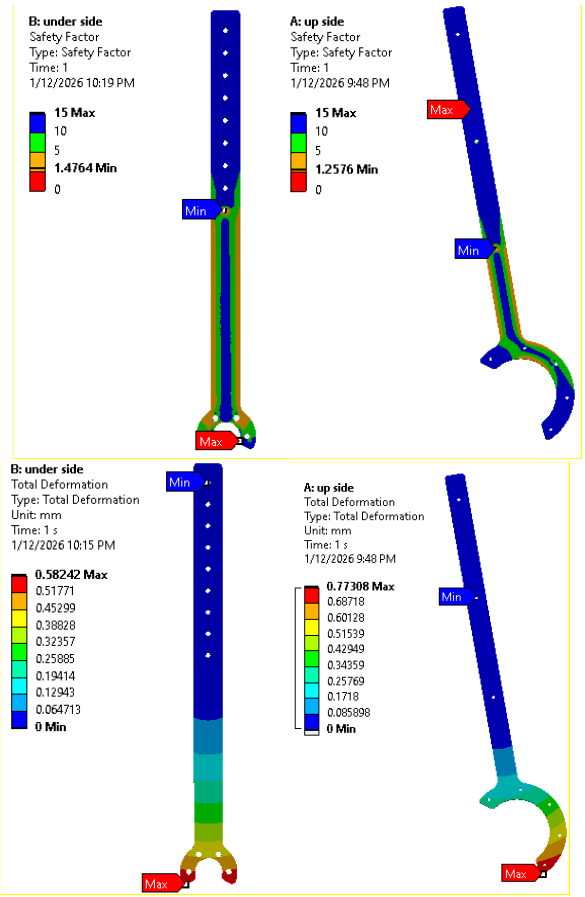

Fig. 3 Finite-element results for the actuator–orthosis links under a 30 N·m knee-axis torsional moment. Top: yield-based safety factor distributions for the shank link (B) and the thigh link (A). Bottom: total deformation distributions (mm) for the same links.

2-3- Finite State Machine

The overall behavior of the device is organized as a finite state machine with four main modes: Sitting, Standing, Walking, and Knee-exercise (Fig. 4). At initialization, the system selects either the Sitting or Standing state depending on the measured knee angle from the encoder (whichever posture is closer). Starting from the Sitting state, the therapist can either command a transition to Standing or activate the Knee-exercise mode. In the Knee-exercise mode, the user remains seated while the actuator repeatedly drives the joint through a predefined flexion–extension pattern around a comfortable neutral angle; the exercise speed can be increased or decreased in real time using dedicated buttons on the hand-held terminal, and cancelling this mode returns the system to Sitting. From the Sitting state, a transition to Standing is also possible, and the user can toggle back from Standing to Sitting when required. In the Standing state, the therapist may command the device to enter the Walking mode, in which the high-level controller continuously generates a periodic knee trajectory for overground gait. During Walking, both the cycle duration (interpreted as walking speed) and the swing-phase flexion amplitude (step height) can be adjusted online from the same interface. The Walking mode is maintained until a stop command is issued from the terminal, which returns the system to the Standing state and disables the cyclic motion.

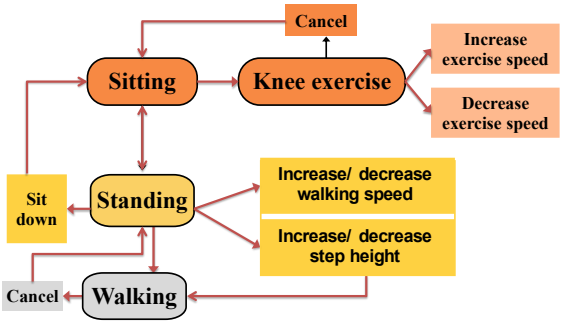

Fig. 4 State-machine architecture illustrating the sitting, standing, walking, and knee-exercise modes and the transitions between them.

2-4- Embedded Control Framework

The powered knee joint is controlled using a hierarchical two-level architecture as shown in Fig.1 (d). A high-level loop running on the main controller generates the desired knee trajectory according to the selected operating mode and user-defined parameters, while a low-level loop embedded in the actuator executes the commanded motion at the joint. User commands are issued on the touchscreen hand terminal based on an STM32F469 microcontroller, where the operating mode and the discrete step-height and step-speed levels are selected. These commands are then transmitted to the main controller (STM32F429 Discovery) via a USART link.

The high-level control loop is implemented in MATLAB/Simulink and automatically deployed to the STM32F429 controller using the Waijung code-generation framework. This block receives the mode and user commands from the touchscreen terminal (step-height level and step-speed level) and, based on the current state of the finite state machine, generates the corresponding knee motion pattern, which is then forwarded to the low-level actuator controller. Before detailing the interface signals between the two levels, the underlying knee reference pattern and its scaling must be described.

For the high-level controller, the knee motion is represented as a function of a normalized gait phase g. Following the swing trajectories proposed by [23], the base reference pattern $\theta_{\text{base}}(g)$ is defined by an analytic expression over $g \in [0,1]$ with distinct swing and stance sub-intervals. This phase-based representation provides a compact and differentiable description of the desired knee motion, which is particularly convenient for subsequent scaling with respect to step height and step speed.

The analytical expression of $\theta_{\text{base}}(g)$ is given in (1), and the corresponding profile, together with the swing and stance sub-intervals, is illustrated in Fig. 5.

$$\theta_{base}(g) = \begin{cases} \theta_0 + \frac{k_a}{2}\left[1 - cos\left(2\pi \frac{g}{g_{sw}}\right)\right], & 0 \le g \le g_{sw} \\ \theta_0, & g_{sw} < g \le 1 \end{cases} \quad (1)$$

In this study, the swing–stance boundary was chosen such that approximately 20% of the cycle is assigned to swing and the remaining 80% to stance, as illustrated in Fig. 5. This choice reflects the participant's baseline gait with the conventional KAFO. After placing the swinging foot on the ground, he did not immediately

initiate swing of the contralateral limb. Instead, he shifted the trunk backward into a compensatory hip–trunk hyperextension and required extra stance time to regain stability before the next step. Similar compensatory trunk and hip hyperextension patterns are commonly observed in individuals with SCI walking with KAFOs.

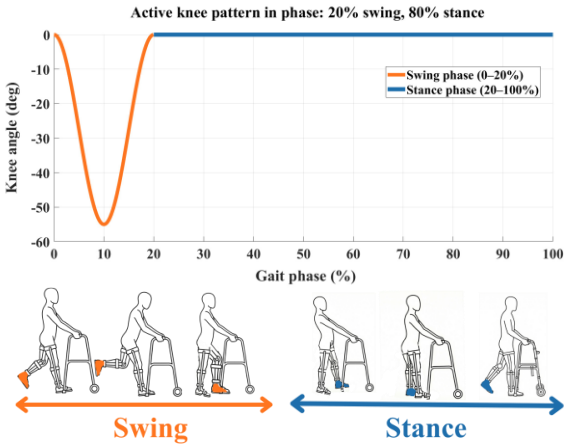

Fig. 5 Knee angle pattern with 20% swing and 80% stance, with schematic snapshots of the user during the swing and stance phases.

In (1), the normalized gait phase g denotes the progression through a gait cycle between two consecutive heel-strike events of the assisted limb. In this formulation, the sub-interval $[0, g_{\text{sw}}]$ corresponds to the swing phase, during which the knee follows a smooth flexion–extension profile, while the sub-interval $[g_{\text{sw}}, 1]$ represents stance, where the reference angle is kept close to an almost constant extension level. The constant term θ_0 in (1) defines a baseline knee flexion and accounts for the fact that, in individuals with spinal cord injury, full anatomical extension may not be achievable (e.g. due to contracture), so that the reference trajectory never enforces a perfectly straight knee.

The parameter k_a in (1) sets the flexion amplitude of the swing phase and therefore determines the step height generated by the orthosis. In the current implementation, k_a is chosen from four discrete levels, $k_a \in \{0.75, 1.0, 1.25, 1.5\}$. On the touchscreen terminal, these levels are presented to the therapist simply as qualitative options ranging from "minimum" to "maximum" step height, so that selecting a higher level monotonically increases the peak knee flexion while preserving the overall shape and timing of the reference pattern.

In addition to step height, the controller allows the user to adjust step speed by modulating the evolution of the gait phase rather than changing the spatial shape of $\theta_{\text{base}}(g)$. Four discrete step-speed modes $m \in \{1,2,3,4\}$ are available on the touchscreen terminal. Each mode is mapped to a positive phase-speed scaling factor $\sigma(m) \in \{0.75, 1, 1.5, 2\}$ so that higher modes correspond to faster progression through the gait cycle. For a given mode m, a ramp-shaped phase-speed profile $s(g; m)$ is defined over the normalized gait phase g. During swing ($0 \le g \le g_{\text{sw}}$), the factor increases linearly from 1 to σ_m:

$$s_{\text{sw}}(g; m) = 1 + (\sigma_m - 1)\,\frac{g}{g_{\text{sw}}} \tag{2}$$

whereas during stance ($g_{\text{sw}} < g \le 1$) it decreases linearly from σ_m back to 1:

$$s_{\text{st}}(g; m) = \sigma_m + (1 - \sigma_m)\,\frac{g - g_{\text{sw}}}{1 - g_{\text{sw}}} \tag{3}$$

The complete phase-speed modulation is then given by:

$$s(g; m) = \begin{cases} s_{\text{sw}}(g; m), & 0 \le g \le g_{\text{sw}}, \\ s_{\text{st}}(g; m), & g_{\text{sw}} < g \le 1. \end{cases} \tag{4}$$

The dynamics of the phase are finally defined as

$$\frac{dg}{dt} = v_0\, s(g; m) \tag{5}$$

with $v_0 > 0$a nominal phase velocity. In this way, changing the step-speed mode results in a smooth, cycle-wise modification of phase velocity (accelerating the progression through swing and decelerating it back during stance) rather than abrupt jumps in gait timing, which is beneficial for both actuator behavior and user comfort.

Following the description of the high-level trajectory generation, the low-level controller is considered, beginning with its inputs and outputs. As summarized in Fig. 1(d) the high-level board sends the following command data to the actuator, via the CAN bus, where p_{des} is the desired knee angle obtained from the phase-based trajectory, v_{des} is the desired angular velocity, K_p and K_d are the stiffness and damping gains, and τ_{ff} is an optional feed-forward torque term. In the opposite direction, the low-level controller returns the measured joint angle θ_m and angular velocity $\dot{\theta}_m$, both derived from the motor encoder and coinciding with the mechanical knee motion; these signals are used in the high-level loop to monitor the joint behavior and the evolution of the assisted gait.

At joint level, the actuator operates in the manufacturer's so-called MIT mode, which implements a joint-level PD impedance controller as:

$$\tau_{\text{ref}} = K_p(p_{\text{des}} - \theta_m) + K_d(v_{\text{des}} - \dot{\theta}_m) + \tau_{ff} \tag{6}$$

In this mode, the commanded torque τ_{ref} is generated from the position and velocity error, through the stiffness and damping gains K_p and K_d, so that the knee behaves as a virtual spring–damper system anchored to the desired trajectory. In the present study, we deliberately use a simplified configuration in which the desired velocity and feed-forward torque inputs are not exploited ($v_{\text{des}} = 0,\ \tau_{ff} = 0$); the motion is therefore driven primarily by the position-related impedance terms, with the damping term acting against the measured joint velocity to stabilize the movement around the reference.

The gains K_p and K_d are adjusted on a subject-specific basis during supervised tuning sessions. Starting from conservative nominal values, they are increased until an acceptable compromise is obtained between accurate tracking of the swing pattern (sufficient stiffness to reproduce the reference trajectory) and comfortable interaction (sufficient compliance to allow the user's residual hip and trunk motions to contribute to the movement rather than being overridden by the actuator).

2-5- Experimental Methods

In the implementation phase, the proposed active KAFO was tested on a spinal cord injury patient who routinely walked with a conventional KAFO and a walker in daily life as shown in Fig. 1(a). The main clinical characteristics of this participant are summarized in Table 2. The device is primarily intended for individuals with incomplete SCI who retain sufficient trunk stability and some residual hip control, and who typically offload body weight using a walker during ambulation.

Two orthotic configurations were tested. In the passive configuration, both the right and left legs were fitted with the participant's usual conventional KAFOs, with the knees locked in extension and the ankles fixed in the alignment used in daily life.

Table 2 Clinical and physical characteristics of the SCI participant

Sex (M/F)	Age (years)	Height (cm)	Body mass (kg)	Neurological level of injury	AIS grade	Time since injury (years)
M	25	188	82	T1	C	9

In the active configuration, the left leg was fitted with the active KAFO, while the right leg continued to use the conventional KAFO. During two 60-minute practice sessions, the participant walked with the active device while the operator adjusted the step height and step

speed on the on-board interface; the final parameter set was chosen according to the participant's comfort and was then kept fixed for all active-condition tests. In both configurations, the ankles remained locked and the participant used the walker and footwear as in daily life.

The participant presented spasticity in the knee flexor and extensor muscles. Therefore, at the beginning of each session— including both the practice sessions and the final evaluation session—a 15-minute seated exercise was performed in which the device repeatedly flexed and extended the knee with a cyclic pattern. Only after this preparatory phase did the participant stand up and start the walking tests. Passive and active configurations were evaluated in separate sessions, approximately one week apart.

All walking tests were performed indoors on a straight, level corridor of approximately 10m. The protocol included the 10-meter walking test (10MWT) and the 6-minute walking test (6MWT) in both configurations, with at least 20 minutes of rest between tests.

For the 10MWT, a 10m path was marked on the floor. The participant was instructed to walk at a comfortable self-selected speed using his walker. Walking time was measured, starting when the first foot crossed the start line and stopping when it crossed the finish line. Each condition (passive and active) was tested twice, and the average walking speed was obtained as distance divided by the mean time over the two trials.

For the 6MWT, the participant repeatedly walked along the length of the corridor for 6 minutes at a comfortable pace, turning around at markers placed at each end. The total distance covered after 6 minutes was determined from floor markings and measuring tape. In the active configuration, when approaching the turning points, the step-speed parameter could be slightly reduced online via the on-board interface to facilitate safe turning before resuming the previous speed. The participant was allowed to slow down or briefly stop if needed, and any such events were noted. Each condition was tested twice in the 6MWT, and the mean distance over the two trials was used for analysis. All tests were performed under the supervision of a physiotherapist or clinician, with the patient's informed consent and in accordance with the relevant faculty regulations.

3- Results and Discussion

In this section, first the implemented knee reference pattern and parameter settings in the active configuration are described, and then the clinical walking test results are presented.

3-1- Results

Fig. 6 illustrates the implemented knee-angle reference over one gait cycle for four speed levels used in the active configuration. The waveform follows the cosine-like trajectory defined in equation (1), with $k_a = 1.25$ applied to set the final step height. Speed modulation was obtained by changing the period of the reference; four discrete speed levels ($m \in \{1,2,3,4\}$) were defined and are shown in Fig. 6 as time-scaled versions of the same profile. During the comparative walking tests, the participant predominantly walked with level 3 (corresponding to $\sigma(m) = 1.5$), while temporarily switching to level 1 (corresponding to $\sigma(m) = 0.75$) when approaching the turning points in the 6MWT to facilitate safer, slower turns.

To illustrate the effort required by the low-level controller to track the predefined knee trajectory, Fig. 7 reports the estimated commanded knee torque over one representative gait cycle, computed from the joint-space PD impedance law described in Section 2-4 using the tracking error between the reference trajectory and the measured knee motion. The profile is shown across stance and swing and highlights the expected phase-dependent demand: lower torque levels are generally required during swing, whereas higher torques are demanded during stance to stabilize the knee and maintain weight-bearing support. The peak commanded torque is on the order of the actuator's maximum capability, indicating that stance stabilization can approach the upper range of the available actuation.

Walking performance in the passive and active configurations is summarized in Table 3. The reported values represent the mean across two repetitions performed in each condition. In the active condition, the 10MWT time decreased from 51 s to 37.6 s (≈26% faster), corresponding to an increase in walking speed from 0.19 m/s to 0.26 m/s (≈37% higher). End-of-test heart rate during the 10MWT remained similar between conditions (115 bpm passive vs 118 bpm active). For the 6MWT, the distance covered was comparable (53.2 m passive vs 54.6 m active, ≈2.6% higher), with a modest increase in end-of-test heart rate (133 bpm passive vs 140 bpm active).

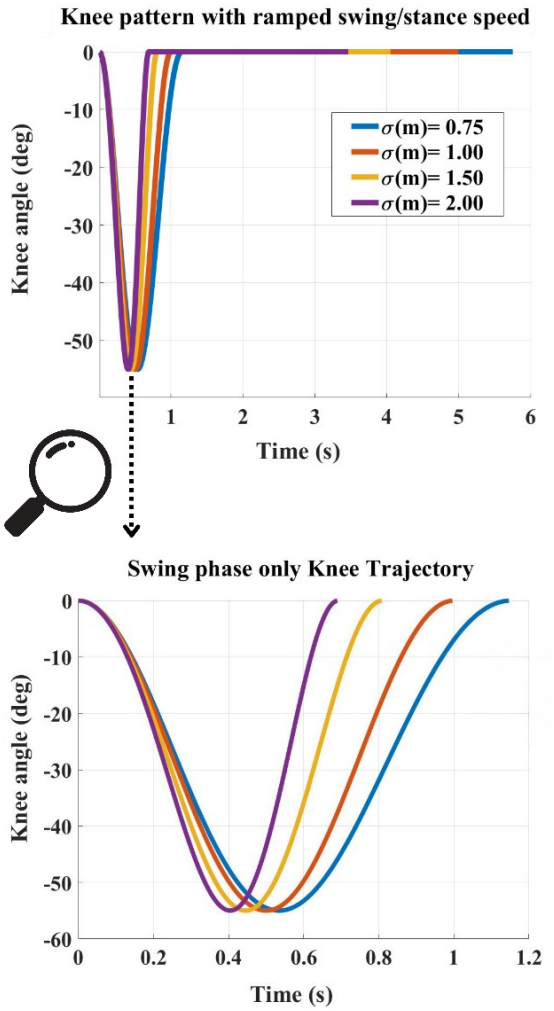

Fig. 6 Knee angle trajectories for four commanded walking speeds: full pattern over one gait cycle with ramped swing/stance timing (top), and zoomed swing-phase profiles illustrating the resulting time-scaling of the knee motion (bottom).

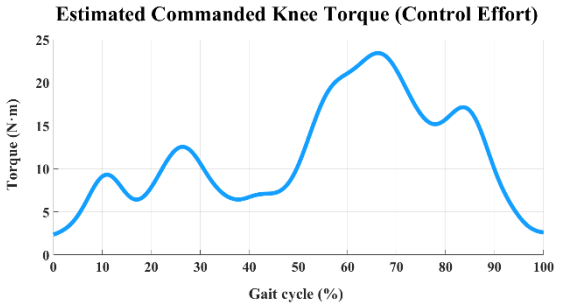

Fig. 7 Estimated commanded knee torque (control effort) over one representative gait cycle, computed from the joint-space PD impedance controller. The swing and stance phases are indicated.

Table 3 6MWT and 10MWT outcome measures under passive and active KAFO conditions

Condition	10MWT time (s)	10MWT speed (m/s)	6MWT distance (m)	HR end of 10MWT (bpm)	HR end of 6MWT (bpm)
Passive	51	0.19	53.2	115	133
Active	37.6	0.26	54.6	118	140

3-2-Discussion

The implemented knee reference pattern was designed not only to reproduce a physiologically inspired flexion–extension profile, but also to allow smooth adjustments of walking speed during use. As shown in Fig. 6, increasing the speed level up to approximately twice the slowest setting led to relatively modest changes in swing duration compared with stance. This design choice was intentional. Because the user can change the speed level while walking, abrupt changes in the timing of the reference could destabilize the gait, especially in a spinal cord injured individual relying on a walker and with limited trunk control. By keeping the stance phase comparatively conservative and distributing most of the timing changes over the whole cycle in a ramp-like manner, the controller aimed to avoid sudden accelerations of the knee and to preserve overall stability during weight-bearing.

In addition, the reference was shaped such that knee extension during late swing occurred slightly faster than knee flexion in early swing as shown in Fig. 6. This asymmetric timing was motivated by a clinical rationale: a quicker extension phase may facilitate projection of the leg forward and help the user clear the foot and prepare for heel contact with less compensatory motion at the trunk and upper limbs. Although the present single-case study does not allow this hypothesis to be formally tested, the participant was able to walk comfortably with this pattern and to modulate speed during everyday-like tasks such as corridor turning. In the active configuration, he could transiently reduce the speed level when approaching a turning point and then return to his preferred level without stopping, suggesting that the on-board interface and the underlying parametric trajectory were practical and intuitive enough to be used during continuous walking.

In terms of functional walking performance, the active configuration provided a clear benefit over the conventional orthosis in the short-distance test. As shown in Table 3, the 10MWT time was reduced and the corresponding walking speed increased when the active KAFO was used. This suggests that adding controlled knee flexion–extension during swing can help the user move more efficiently over short distances, which are typical of many everyday indoor tasks such as walking along a corridor or between rooms. End-of-test heart rate in the 10MWT remained in a similar range in both configurations, indicating that the higher speed in the active condition was not accompanied by a disproportionate increase in cardiovascular effort.

In contrast, no clear difference was observed in the 6MWT distance between the two configurations. During the 6MWT the participant requested more frequent rests in the active condition. This behavior may be related to the limited familiarization with the active device (two one-hour sessions) compared with the long-term use of the conventional KAFO, and to an initial anxiety about relying on the powered knee, which could have led to overuse of upper limbs and fatigue earlier than strictly necessary. Moreover, in a 6-minute test the limiting factors are not restricted to the knee mechanics but also include trunk stability, upper-limb endurance while using the walker, and overall confidence with the new device. The combination of these factors could help explain why the active KAFO produced a marked improvement in short-distance walking speed but no evident change in endurance over six minutes.

Relative to previously reported active KAFO prototypes for people with SCI, the present system makes several practical advances.

- Instead of being evaluated mainly on healthy subjects [19, 22, 23] or in highly constrained set-ups such as parallel bars controlled from an external computer [21], this device was tested on a chronic SCI user who routinely walks with a KAFO and a walker, in a simple corridor environment that is closer to everyday clinical use.
- The on-board touchscreen interface enables straightforward personalization of step height and speed over a few sessions based on patient feedback, without the need for complex software tools, making the tuning process more accessible to users.
- The proposed ramp-based strategy for scaling the knee reference in time provides smooth changes in speed while avoiding abrupt shifts in the timing of flexion–extension, which is desirable for a user with limited trunk control and reliance on a walker.
- The knee actuator is backdrivable and controlled in a position-based impedance mode, which facilitates physical interaction with users who retain some residual motor function and allows them to contribute actively to the movement rather than being fully driven by the mechanism.
- The finite state machine implemented on the controller includes not only walking states but also modes for seated knee exercise and sit-to-stand transitions, which are directly relevant for managing spasticity and preparing the limb before gait training.

Despite these advantages, the present work has some limitations. The results come from a single case with low-level incomplete SCI, so they should be interpreted as preliminary and not generalized to the broader SCI population. Accordingly, no claims of population-level generalizability are made in this study. The tests were carried out in a simple indoor, level environment, and the assessment focused on basic clinical measures (10MWT, 6MWT and end-of-test heart rate) rather than more detailed biomechanical analyses. In addition, although the device supports sit-to-stand transitions, these trials were performed in the context of aided ambulation (e.g., using a walker/crutch), and fully unaided sit-to-stand can require higher knee torques than those available with the current actuator.

Future work should therefore involve a larger cohort of participants with different lesion levels and functional capacities (e.g., including incomplete thoracic and lumbar injuries). It should also assess a bilateral active configuration in more varied and challenging walking tasks and include longer training periods to better capture adaptation to the device. Future studies will also investigate the device behavior under involuntary muscle spasms (spasticity) and evaluate the robustness of the control strategy in such events. It would also be valuable to complement the current parametric knee trajectory with subject-specific reference patterns derived from musculoskeletal modelling and optimization, and to adopt richer outcome measures combining biomechanical analysis with questionnaires on comfort, perceived stability and usability.

4- Conclusion

In this work, we designed and implemented a lightweight active KAFO for individuals with spinal cord injury, featuring a backdrivable knee actuator controlled in a position-based impedance mode and a parametric knee reference whose step height and speed can be adjusted in real time via an on-board touchscreen interface. A pilot evaluation on a single participant with chronic low-level incomplete SCI suggested that, compared with his conventional rigid KAFO, the active configuration could improve short-distance functional walking, as reflected by a higher 10MWT speed, without a marked increase in end-of-test heart rate, while no clear difference was observed in 6MWT distance.

These preliminary findings indicate that a lightweight active KAFO with an adjustable knee trajectory may offer a viable intermediate option between conventional rigid braces and full lower-limb exoskeletons for selected SCI users, retaining the mechanical stability and simplicity of a KAFO while providing controlled knee motion during swing and practical on-device tuning of gait parameters.

Ethics Approval:
The scientific content of this article is the result of the authors' research and has not been published in any Iranian or international journal.

Conflict of Interest:
There are no conflicts of interest to declare.

References

[1] N. Sezer, S. Akkuş, and F. G. Uğurlu, "Chronic complications of spinal cord injury," *World journal of orthopedics,* vol. 6, no. 1, p. 24, 2015, doi: 10.5312/wjo.v6.i1.24.

[2] N. S. C. I. S. Center, "Facts and Figures at a Glance," *Birmingham, AL: University of Alabama at Birmingham,* vol. 10, 2016. [Online]. Available: https://www.scirepair.com/uploads/8/6/1/5/86150236/spinal_cord_injury_facts_and_figures_at_a_glance_2017.pdf.

[3] R. A. Auberger, "Functional Compensation of Gait Deficits with Minimal Actuation," ETH Zurich, 2021. [Online]. Available: https://www.research-collection.ethz.ch/server/api/core/bitstreams/7e7aecd0-a74f-4a27-a94c-73ec97a32683/content

[4] T. Yakimovich, E. D. Lemaire, and J. Kofman, "Engineering design review of stance-control knee-ankle-foot orthoses," *Journal of Rehabilitation Research & Development,* vol. 46, no. 2, 2009, doi: 10.1682/JRRD.2008.02.0024.

[5] K. Ghoseiri and A. Zucker-Levin, "Long-term locked knee ankle foot orthosis use: A perspective overview of iatrogenic biomechanical and physiological perils," *Frontiers in Rehabilitation Sciences,* vol. 4, p. 1138792, 2023, doi: doi.org/10.3389/fresc.2023.1138792.

[6] M. J. Escalona *et al.*, "Cardiorespiratory demand and rate of perceived exertion during overground walking with a robotic exoskeleton in long-term manual wheelchair users with chronic spinal cord injury: A cross-sectional study," *Annals of physical and rehabilitation medicine,* vol. 61, no. 4, pp. 215-223, 2018, doi: 10.1016/j.rehab.2017.12.008.

[7] J. Kressler, T. Wymer, and A. Domingo, "Respiratory, cardiovascular and metabolic responses during different modes of overground bionic ambulation in persons with motor-incomplete spinal cord injury: A case series," *Journal of Rehabilitation Medicine (Stiftelsen Rehabiliteringsinformation),* vol. 50, no. 2, 2018, doi: 10.2340/16501977-2281.

[8] A. Plaza, M. Hernandez, G. Puyuelo, E. Garces, and E. Garcia, "Wearable rehabilitation exoskeletons of the lower limb: analysis of versatility and adaptability," *Disability and Rehabilitation: Assistive Technology,* vol. 18, no. 4, pp. 392-406, 2023, doi: 10.1080/17483107.2020.1858976.

[9] D. Herrera-Valenzuela *et al.*, "A qualitative study to elicit user requirements for lower limb wearable exoskeletons for gait rehabilitation in spinal cord injury," *Journal of NeuroEngineering and Rehabilitation,* vol. 20, no. 1, p. 138, 2023, doi: 10.1186/s12984-023-01264-y.

[10] M. Laffranchi *et al.*, "User-Centered design and development of the modular TWIN lower limb exoskeleton," *Frontiers in neurorobotics,* vol. 15, p. 709731, 2021, doi: 10.3389/fnbot.2021.709731.

[11] S. H. Kwon *et al.*, "Energy efficiency and patient satisfaction of gait with knee-ankle-foot orthosis and robot (ReWalk)-assisted gait in patients with spinal cord injury," *Annals of rehabilitation medicine,* vol. 44, no. 2, pp. 131-141, 2020, doi: 10.5535/arm.2020.44.2.131.

[12] A. Rodríguez-Fernández, J. Lobo-Prat, R. Tarragó, D. Chaverri, X. Iglesias, and L. Guirao-Cano, "Comparing walking with knee-ankle-foot orthoses and a knee-powered exoskeleton after spinal cord injury: a randomized, crossover clinical trial.," *Scientific reports,* vol. 12, 2022, doi: 10.1038/s41598-022-23556-4.

[13] M. Arazpour, A. Chitsazan, M. A. Bani, G. Rouhi, F. T. Ghomshe, and S. W. Hutchins, "The effect of a knee ankle foot orthosis incorporating an active knee mechanism on gait of a person with poliomyelitis," *Prosthetics and orthotics international,* vol. 37, no. 5, pp. 411-414, 2013, doi: 10.1177/0309364612469140.

[14] G. S. Sawicki and D. P. Ferris, "A pneumatically powered knee-ankle-foot orthosis (KAFO) with myoelectric activation and inhibition," *Journal of neuroengineering and rehabilitation,* vol. 6, no. 1, p. 23, 2009, doi: 10.1186/1743-0003-6-23.

[15] G. Puyuelo-Quintana *et al.*, "A new lower limb portable exoskeleton for gait assistance in neurological patients: a proof of concept study," *Journal of NeuroEngineering and Rehabilitation,* vol. 17, no. 1, p. 60, 2020, doi: 10.1186/s12984-020-00690-6.

[16] M. S. Ashrafi, M. Nazari, N. Sepehry, M. Mahdizadeh Rokhi, P. Samimi, and M. Attarchi, "Design and implementation of a fuzzy output feedback assistive controller for a series-elastic-actuator-driven knee exoskeleton," *Modares Mechanical Engineering,* vol. 22, no. 8, pp. 541-553, 2022, doi: 10.52547/mme.22.8.541.

[17] J. de Miguel Fernandez *et al.*, "Adapted assistance and resistance training with a knee exoskeleton after stroke," *IEEE Transactions on Neural Systems and Rehabilitation Engineering,* vol. 31, pp. 3265-3274, 2023, doi: 10.1109/TNSRE.2023.3303777.

[18] C. Meijneke *et al.*, "Symbitron exoskeleton: Design, control, and evaluation of a modular exoskeleton for incomplete and complete spinal cord injured individuals," *IEEE Transactions on Neural Systems and Rehabilitation Engineering,* vol. 29, pp. 330-339, 2021, doi: 10.1109/TNSRE.2021.3049960.

[19] C. Nesler, G. Thomas, N. Divekar, E. J. Rouse, and R. D. Gregg, "Enhancing voluntary motion with modular, backdrivable, powered hip and knee orthoses," *IEEE robotics and automation letters,* vol. 7, no. 3, pp. 6155-6162, 2022, doi: 10.1109/LRA.2022.3145580.

[20] J. Kazemi and S. OZGOLI, "Parametric model of human constrained gait with implementation on exoped exoskeleton," *Modares Mechanical Engineering,* vol. 18, no. 6, pp. 12-18, 2018. [Online]. Available: https://mme.modares.ac.ir/article_10442_890ff058169b5a1d1a7f07d467f1f57b.pdf.

[21] J. M. Font-Llagunes, U. Lugrís, D. Clos, F. J. Alonso, and J. Cuadrado, "Design, control, and pilot study of a lightweight and modular robotic exoskeleton for walking assistance after spinal cord injury," *journal of Mechanisms and Robotics,* vol. 12, no. 3, p. 031008, 2020, doi: 10.1115/1.4045510.

[22] D. García-Vallejo, J. M. Font-Llagunes, and W. Schiehlen, "Dynamical analysis and design of active orthoses for spinal cord injured subjects by aesthetic and energetic optimization," *Nonlinear dynamics,* vol. 84, no. 2, pp. 559-581, 2016, doi: 10.1007/s11071-015-2507-1.

[23] M. Febrer-Nafría, B. J. Fregly, and J. M. Font-Llagunes, "Evaluation of optimal control approaches for predicting active knee-ankle-foot-orthosis motion for individuals with spinal cord injury," *Frontiers in Neurorobotics,* vol. 15, p. 748148, 2022, doi: 10.3389/fnbot.2021.748148.

[24] "Cubemars, "AK80-8 KV60 robotic actuator," Cubemars,." [Online]. Available: https://www.cubemars.com/product/ak80-8-kv60-robotic-actuator.html.